Traffic Sign Detection via Graph-Based Ranking and Segmentation Algorithms

Xue Yuan, *Member, IEEE*, Jiaqi Guo, Xiaoli Hao, and Houjin Chen

***Abstract*—The majority of existing traffic sign detection systems utilize color or shape information, but the methods remain limited in regard to detecting and segmenting traffic signs from a complex background. In this paper, we propose a novel graph-based traffic sign detection approach that consists of a saliency measure stage, a graph-based ranking stage, and a multithreshold segmentation stage. Because the graph-based ranking algorithm with specified color and saliency combines the information of color, saliency, spatial, and contextual relationship of nodes, it is more discriminative and robust than the other systems in terms of handling various illumination conditions, shape rotations, and scale changes from traffic sign images. Furthermore, the proposed multithreshold segmentation algorithm focuses on all the nodes with a nonzero ranking score, which can effectively solve problems such as complex background, occlusion, various illumination conditions, and so on. The results for three public traffic sign sets show that our proposed approach leads to better performance than the current state-of-the-art methods. Moreover, the results are satisfactory even for images containing traffic signs that have been rotated or undergone occlusion, as well as for images that were photographed under different weather and illumination conditions.**

***Index Terms*—Graph-based image analysis, graph-based image segmentation, traffic sign detection.**

I. Introduction

CURRENTLY, more and more intelligent transportation systems are developed for assisting drivers [1]–[13]. Traffic sign recognition (TSR) is extremely important for safe and careful driving, as not only can this system inform the driver of the conditions of the road, but can also support the driver during the tedious task of remembering each of the many types of traffic signs. Some of the traffic sign information may sometimes be extracted from the GPS navigation data, but it is always neither complete nor up-to-date. Moreover, temporary speed limits for road works, as well as variable speed limits, are by registration not included in predefined digital cartographic data. Therefore, a visual real-time TSR system is a mandatory complement to GPS systems for designing advanced driving assistance systems.

Traffic signs are designed using specific shapes and colors, which are highly salient and visible from the background against which they are set, enhancing their visibility to drivers. In-depth study of traffic sign datasets allows us to observe some common characteristics of traffic signs.

1) Traffic signs are designed with specified colors (i.e., red, blue, yellow, or white).
2) Traffic signs are highly salient.
3) The image intensities in traffic sign regions present appearance coherence.

In this paper, we propose a novel graph-based ranking and segmentation approach to detect salient regions, with specified colors, as traffic sign candidate regions. The proposed approach combines information pertaining to the color, saliency, spatial, and contextual relationship of nodes for traffic sign detection, making it more discriminative and robust than other methods in addressing various illumination conditions, shape rotations, and scale changes of traffic sign images.

The remainder of this paper is organized as follows. In Section II, we review previous research, and describe our improvement on this. Section III presents a novel graph-based ranking and segmentation algorithms for traffic sign detection system. Section IV presents a support vector machine (SVM) classifier for traffic sign classification. We present our experimental results in Section V. The conclusion is given in Section VI.

II. Related Research and Contributions

A. Related Research

A TSR system usually involves two main steps.

1) *The Traffic Sign Detection Stage:* Detection of potential traffic signs in the image.
2) *The TSR Stage:* Classification of the selected regions of interest (ROI) for identifying the exact type of traffic sign, or rejecting the ROI.

In the traffic sign detection stage, the majority of systems make use of color information as a method for detecting an image. The performance of color-based traffic sign detection is often reduced in scenes that have strong illumination, poor lighting, or adverse weather conditions. Color models have been used in an attempt to overcome these problems. For example, Gao *et al*. [1] proposed a TSR system based

Manuscript received October 15, 2014; revised December 20, 2014; accepted February 7, 2015. Date of publication June 1, 2015; date of current version November 13, 2015. This work was supported in part by the Specialized Research Fund for the Doctoral Program of Higher Education under Grant 20110009120003 and Grant 20110009110001, in part by the National Natural Science Foundation of China under Grant 61301186 and Grant 61271305, and in part by the School Foundation of Beijing Jiaotong University under Grant 2010JBZ010 and Grant 2015JBM019. This paper was recommended by Associate Editor M. Celenk.

The authors are with the School of Electronic and Information Engineering, Beijing Jiaotong University, Beijing 100044, China (e-mail: xyuan@bjtu.edu.cn).

Color versions of one or more of the figures in this paper are available online at http://ieeexplore.ieee.org.

Digital Object Identifier 10.1109/TSMC.2015.2427771

on the extraction of the red and blue regions in the international commission on illumination 1997 color appearance model (CIECAM97) color model. In [2] and [3], the hue and saturation threshold (HST) technique was presented and generalized for red, blue, and yellow. The HST color space has two color components, namely hue and saturation, which are closely related to human perception, and an illumination component that is close to brightness. Prieto and Allen [4] detected potential traffic signs by means of the distribution of red pixels within the image in the YUV color model. In [27] and [29], Moreno *et al*. indicated that the best color-based segmentation algorithm for traffic sign detection is the RGB normalized thresholding (RGBNT) algorithm.

In contrast, several approaches completely ignore color information, and use only shape information from gray scale images. For example, Loy [5] proposed a system that used local radial symmetry to highlight the points of interest in each image, and detected octagonal, square, and triangular traffic signs. Houben [6] established a novel probabilistic measure for traffic sign color detection, based on the color pixels found in their system, and adopted a Hough-like algorithm for detecting circular and triangular shapes. To obtain the likelihood of each pixel being the color of the traffic sign, Houben [6] assumed traffic color distribution to be a mixture of Gaussians, with the averaged colors as means, and a standard deviation of 0.1. Finally, he used the gradient image for voting schemes with the magnitude for each pixel. Xu [7] proposed a novel approach for recognition of various traffic sign shapes using geometric matching.

More recently, Greenhalgh and Mirmehdi [11] and Yuan *et al*. [8] focused on the local stability of traffic sign regions. They proposed a traffic sign detection algorithm using a novel application of maximally stable extremal regions (MSERs), and proved that the MSERs were robust to variations in both lighting and contrast. In addition, some recent systems utilize the sliding window paradigm [9], [10], [12] to detect traffic sign regions. For example, as presented in [10], the original image is resized by a scaling factor s_i to obtain the image corresponding to the pyramid level i. Then, given a pyramid level, they shift the search window along the horizontal and vertical directions based on a histogram of oriented gradient (HOG) and SVM algorithm.

In the TSR stage, the majority of the systems make use of local features and classifiers, such as HOG or scale-invariant feature transform, as well as Haar-like features, for TSR. For example, Ruta *et al*. [9] extracted Haar-like and HOG features from traffic sign images, and Li *et al*. [12] proposed a TSR system using Haar-like features and an adaboost classifier. Yuan *et al*. [8] proposed a novel descriptor to describe an ROI, namely, color global and local oriented edge magnitude patterns (Color Global LOEMP). The Color Global LOEMP is a framework that is able to effectively combine color, global spatial structure, global direction structure, and local shape information, and balance the two concerns of distinctiveness and robustness. A linear SVM classifier was used in [8] to identify the exact type of traffic sign. Lu *et al*. [13] proposed a novel machine learning algorithm called sparse-representation-based graph embedding to strike a balance between local manifold structures and global discriminative information. Different from [8], the primary contribution of this paper is devoted to the traffic sign detection stage.

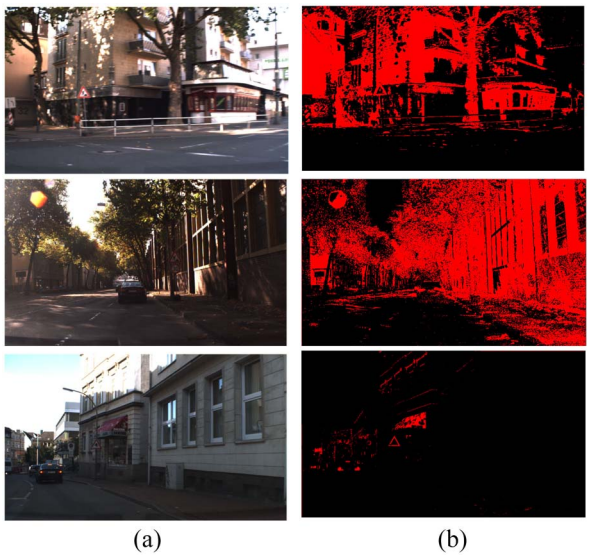

Fig. 1. Examples of using color thresholding method. (a) Input images. (b) Results based on color thresholding method with the same threshold.

B. Limitations of the Related Traffic Sign Detection Systems

Some limitations of the related studies are presented as follows.

1) The performance of color-based traffic sign detection approach is often reduced in setting with adverse weather conditions, such as strong illumination or poor lighting.
2) When the traffic signs have been rotated or occluded, or have undergone affine transformations, the performance of shape-based traffic sign detection method is often reduced.
3) Local features and the sliding window paradigm-based traffic sign detection and recognition method score a large number of windows in a test image using a classifier. Thus, computational complexity and the number of false alarms increase.

C. Contribution

In the detection stage, the majority of the systems utilize color information as a method for segmenting images [1]–[5]. However, fixing thresholds for a traffic sign detection system in outdoor environments is the problem of the color thresholding method. As shown in Fig. 1, if the range of thresholds is large, the number of false alarms increase, otherwise, the number of misses increase. Furthermore, the color thresholding method can only provide a result of either 0 or 1 for each pixel to describe whether or not it is in the traffic sign region. In this paper, we aim at solving the problems of the color-based traffic sign detection method, and propose an algorithm to combine the information of the color, saliency, spatial, and contextual

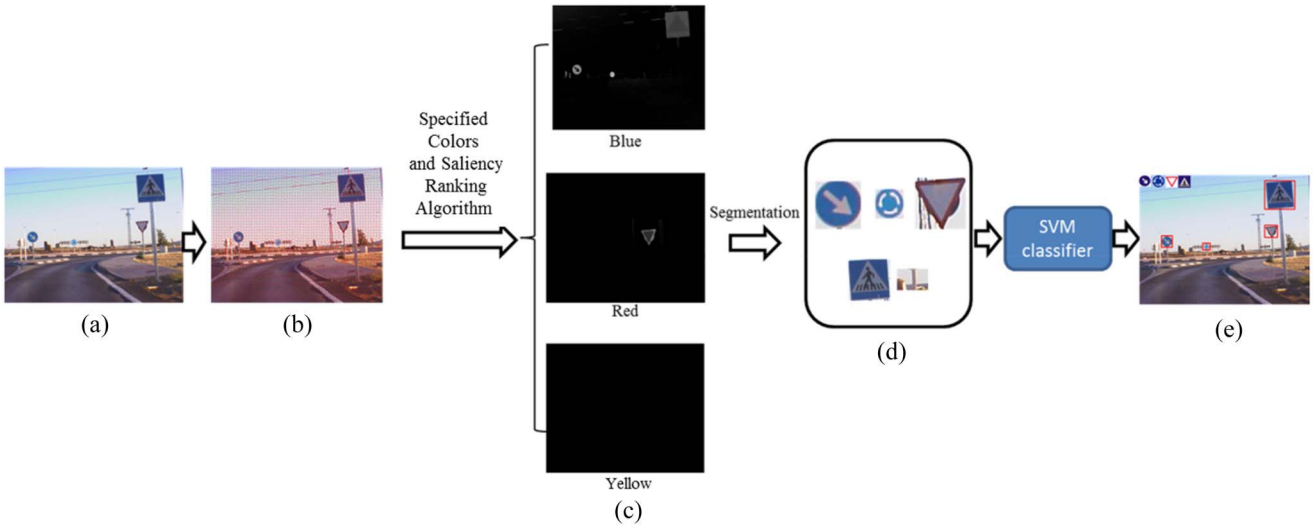

Fig. 2. Flow of proposed traffic sign detection system. (a) Input image. (b) Graph design. (c) Ranking results with specified colors. (d) Segmentation results. (e) Final results of traffic sign detection system.

relationship of nodes for traffic sign detection. Even if we set a wide range of thresholds, false alarms can also be reduced by combining the information of saliency, spatial, or contextual information. Furthermore, a score between 0 and 1 can be given for each node to describe how likely it is to be a part of a traffic sign.

In this paper, graph-based ranking and segmentation algorithms are proposed, which consist of a saliency measure stage, a graph-based ranking stage, and a multithreshold segmentation stage. First, we design a graph to represent an image. We then propose a ranking algorithm to exploit the intrinsic manifold structure of the nodes of the graph, and give each node a ranking score according to its saliency, coherence, and similarity with the specified colors. Finally, we propose a multithreshold segmentation approach to segment traffic sign candidate regions. The key contributions of our algorithm are as follows.

1) A novel graph-based saliency measure algorithm for traffic sign detection is proposed.
2) We provide a novel framework that combines the information of the color, saliency, spatial, and contextual relationship of nodes. It is more discriminative and robust than the other systems in terms of handling various illumination conditions, shape rotations, and scale changes from traffic sign images.
3) The multithreshold segmentation algorithm focuses on all the nodes with a nonzero ranking score, which can effectively solve problems such as complex background, occlusion, various illumination conditions, and so on.

III. Graph-Based Ranking and Segmentation Algorithm for Traffic Sign Detection

Superpixels are generated by the simple linear iterative clustering (SLIC) algorithm [23], which clusters pixels in the combined five-dimensional color and image plane space to efficiently generate compact, nearly uniform superpixels. The flow of our proposed traffic sign detection system is illustrated in Fig. 2. The examples of the superpixels are generated as illustrated in Fig. 3, where Fig. 3(a)–(c) is the examples of 4000, 3000, and 2000 superpixels generated, respectively. De la Escalera *et al.* [14] indicated that a traffic sign is the sum of a color border, a color or achromatic background, and an inner component. To detect small traffic signs, the system must guarantee that the color border of the traffic signs is segmented into independent superpixels. Therefore, in this paper we select 4000 superpixels.

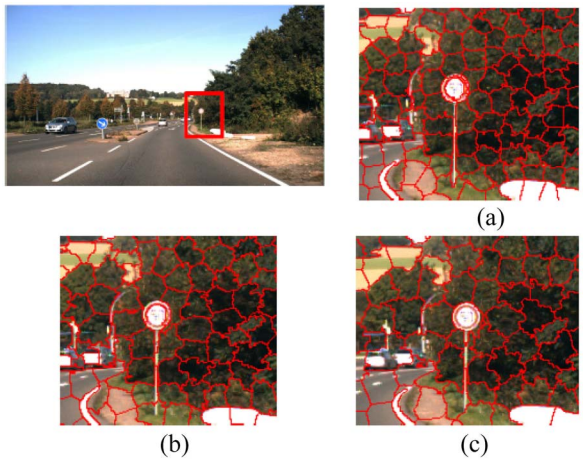

Fig. 3. Examples of superpixels generated with different numbers. Example of (a) 4000, (b) 3000, and (c) 2000 superpixels.

A. Graph Design

We construct a graph $G = (V, E)$, as shown in Figs. 2(b) and 4, in which V is a set of nodes and E is a set of undirected edges. In this paper, each node is a superpixel generated by the SLIC algorithm. To exploit the spatial relationship, we adopted a k-regular graph, which is a graph with vertices of degree k. By extending the scope of node connection with the same degree of k, we effectively utilize the local smoothness cue. Each node is not only connected to

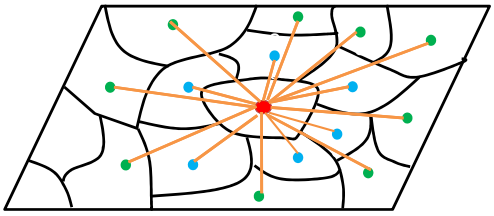

Fig. 4. Graph model. Orange lines link center superpixel and connected nodes [21].

Fig. 5. Examples of superpixels belonging to traffic signs.

its neighboring nodes, but also connected to the nodes sharing common boundaries with these neighboring nodes (see Fig. 4). The weight ω_{ij} connects each pair of nodes i and j, which is defined by the following:

$$\omega_{ij} = \exp\left(-\frac{\|\bar{g}_i - \bar{g}_j\|}{2\sigma^2}\right) \tag{1}$$

where $\bar{g}_i$ denotes the mean color values of the inner pixels of nodes (superpixels) i in the normalized version of RGB color space, respectively, and σ is a constant that controls the strength of the weight. The edges E are weighted by an affinity matrix $W = [\omega_{ij}]_{n\times n}$. With the constraints on the edges, it is clear that the constructed graph is sparsely connected, that is, most elements of the affinity matrix W are zero.

B. Visual Saliency Measure for Each Node

As shown in Fig. 5, each node is a superpixel generated by the SLIC algorithm. V is a set of nodes and E is a set of undirected edges. The neighboring nodes belonging to the background are likely to share similarity appearance, but the nodes belonging to the traffic sign regions have high saliency values. Specifically, for any node i, the saliency is

$$\text{Salient}(i) = \sum_{p=1}^{N} \omega_{ip} \Big/ N \tag{2}$$

where ω_{ip} is a weight connecting each pair of nodes i and p, which can be obtained in (1), and N is the number of the neighboring nodes of node i.

The top TH1 nodes with the largest salient score in an image are considered to be salient nodes. The examples of salient nodes selected in this step are illustrated in Fig. 6. As shown in Fig. 6, almost all the nodes belonging to traffic sign regions have high salient values. The TH1 here is set to 25% by producing the highest F-measure (see Section V-B)

$$S(i) = \begin{cases} 1 & \text{if Salient}(i) \in \text{Top TH1} \quad (3a) \\ 0 & \text{otherwise.} \quad (3b) \end{cases}$$

C. Ranking Algorithm With Specified Colors and Saliency

Yang *et al.* [21] proposed a saliency detection algorithm (SDA) on the basis of graph-based manifold ranking [18], [19], [22]. An image was represented as a close-loop graph with superpixels as nodes. Via graph-based manifold ranking, they consequently ranked these nodes on the basis of their similarity to the background and foreground cues. They conducted saliency detection in a two-stage scheme. First, they used the nodes on the image boundary as background seeds, then constructed four saliency maps using boundary priors, and integrated these for the final map. Consequently, they binary segmented (i.e., salient foreground and background) the saliency map of the first stage, using an adaptive threshold, which facilitated the selection of the nodes of the foreground salient object as queries.

Our goal is to learn a ranking function, which defines the relevance between the nodes of the graph and ranges of the traffic sign colors. The core idea of manifold ranking is to rank the nodes with respect to the intrinsic structure collectively. By taking the relevance between the nodes of the graph and ranges of the traffic sign colors, manifold ranking assigns each node a relative ranking score, instead of an absolute pairwise similarity as traditional ways. In accordance with our aim, we model a traffic sign detection system as a manifold ranking problem. Different from [18]–[22], the proposed traffic sign detection algorithm with manifold ranking requires seeds from several classes, which are initialized with the range of colors of the traffic sign (red, blue, and yellow).

Given a vector $V = \{v_1, \ldots, v_n\} \in \Re^{m\cdot n}$, each element on vector V is a node, and the nodes must be ranked according to their relevance to the objective queries. Let $F : V \to \Re^n$ denote a ranking function that assigns a ranking score, F_i to each node v_i, and F can be viewed as a vector $F = [F_1, \ldots, F_n]^T \in \digamma$. Where T is the symbol of transpose and $\digamma$ denote a set of $n \times 1$ matrices with nonnegative entries. An objective query vector $Y = [Y_1, \ldots, Y_n]^T$ denotes a vector to describe the relationship between the nodes and specified colors.

Based on the properties of traffic signs, the nodes belonging to the traffic sign regions should not change significantly between nearby nodes, nor should they differ significantly from the ranges of the traffic sign colors. The optimal rankings are computed by solving the following optimization problem (4). The cost function associated with F is defined to be

$$\Theta(F) = \arg\min_{F} \frac{1}{2}\left(\sum_{i,j=1}^{n} \omega_{ij} \left\| \frac{F_i}{\sqrt{D_{ii}}} - \frac{F_j}{\sqrt{D_{jj}}} \right\|^2 + \mu \sum_{i=1}^{n} \|F_i - Y_i\|^2\right) \tag{4}$$

where $\mu > 0$ is the regularization parameter, D is the degree matrix with the off diagonal elements, $D_{ii} = \sum_j \omega_{ij}$, and ω is defined in (1). Then the optimization function is

$$F^* = \arg\min_{F\in\digamma} \Theta(F) \tag{5}$$

where the parameter μ controls the balance of the smoothness constraint (the first term) and the fitting

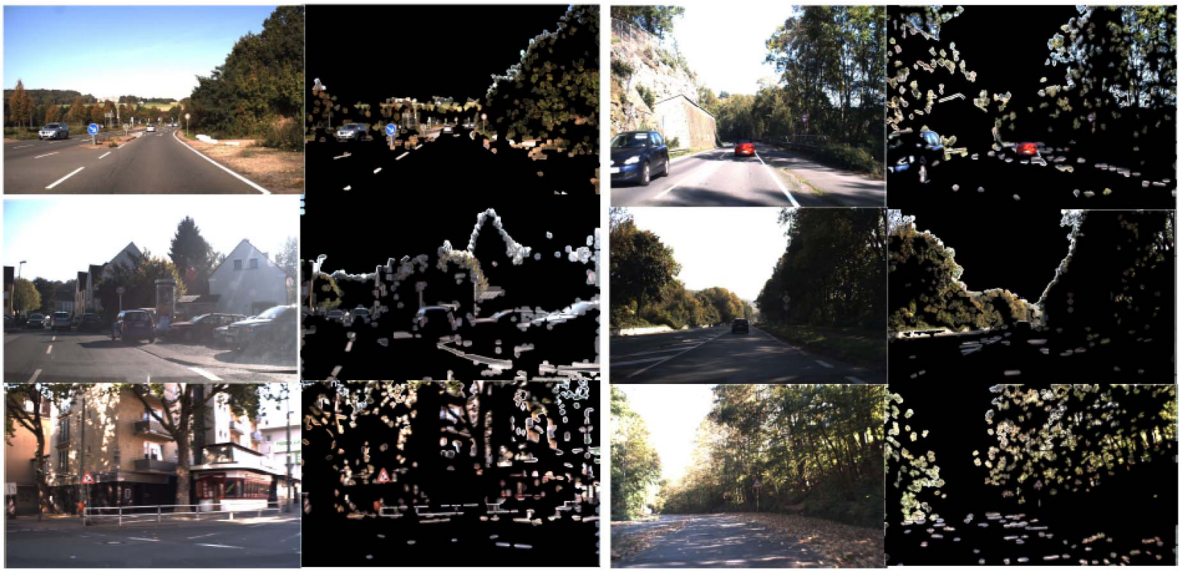

Fig. 6. Examples of nodes with high salient score. (Left) Original image and (right) the nodes with high saliency score.

Fig. 7. Results of ranking algorithm. (a) Original image. (b) Ranking results of original ranking algorithm (11) [21]. (c) Ranking results of proposed algorithm (13).

constraint (second term). A good ranking function should not change too greatly between nearby nodes (the smoothness constraint), nor should it differ too greatly from the objective query assignment (the fitting constraint). The minimum solution is computed by setting the derivative of the above function to be zero. Thus, we have

$$\left.\frac{\partial \Theta}{\partial F}\right|_{F=F^*} = F^* - LF^* + \mu\left(F^* - Y\right) = 0 \tag{6}$$

where L is the normalized Laplacian matrix of the graph, which is constructed by $L = D^{-1/2}WD^{-1/2}$. Equation (6) can be transformed into

$$F^* - \frac{1}{1+\mu}LF^* - \frac{\mu}{1+\mu}Y = 0. \tag{7}$$

Two new variables are introduced here

$$\alpha = \frac{1}{1+\mu} \qquad \beta = \frac{\mu}{1+\mu}. \tag{8}$$

Then

$$(I - \alpha L)F^* = \beta Y. \tag{9}$$

As $(I - \alpha L)$ is invertible, and the scaling factor β does not contribute to our ranking task, (9) is clearly equivalent to

$$F^* = (I - \alpha L)^{-1} Y \tag{10}$$

which recovers the closed form expression of the above iterative algorithm.

In addition, because L is similar to P ($P = D^{-1}W = D^{-1/2}LD^{-1/2}$), we can consider substituting P for L, and then the corresponding closed form is $F^* = (I - \alpha P)^{-1}Y$. It is not difficult to see that this is equivalent to

$$F^* = (D - \alpha W)^{-1} Y \tag{11}$$

where the affinity matrix W is defined by (1) ($W = [w_{ij}]_{n\times n}$ and $D = \text{diag}\{D_{11}, \ldots, D_{nn}\}$).

To combine the information of saliency and contextual relationship of nodes for traffic sign detection, we propose a novel algorithm named specified colors and saliency ranking algorithm. We define a variable Ω as follows:

$$\Omega = (D - \alpha W)^{-1}. \tag{12}$$

By ranking the nodes on the constructed graph, we can regard the inverse matrix Ω in (12) as a complete affinity matrix. This is a nonzero relevance value that exists between any pair of nodes on the graph, and represents the relationships of spatial distances and similarities between any pair of nodes. That is, the relevance between nodes increases when their spatial distance is decreased. The ranking score $F^*(i)$ of the ith node is the inner product of the ith row of Ω and Y. Because Y is a binary vector, $F^*(i)$ can also be viewed as the sum of the relevances of the ith node to the objective query. In this paper, we propose an algorithm to combine the information of saliency and the contextual relationship of nodes as presented in Table I, and obtain a new complete affinity matrix $\hat{\Omega}$, which can describe the information of saliency and spatial, contextual relationship of nodes. The F^* can be rewritten as follows:

$$\hat{F}^* = \hat{\Omega} Y. \tag{13}$$

We set α to 0.9. The threshold α here is set based on experience (see Section V-B).

It is worth noting that this seemingly insignificant process in fact has significant effect on the final results. If we compute the ranking map without setting the nodes having low saliency values to 0, the ranking values of the nodes belonging to large-area regions with specified colors turn abnormally large, so as to severely weaken the contributions of the others to the ranking score.

The ranking vector $\hat{F}^*$ is normalized between the range of 0 and 1 to form the detection result of the first stage

$$\Gamma_{\text{color}}(i) = \overline{\hat{F}^*(i)}. \tag{14}$$

In this paper, we define the objective vector Y in (13) as a binary indicator vector, which indicates whether or not the color value of a node is within the threshold range, as follows:

$$\text{Y}(i) = \begin{cases} 1 & \text{if } \overline{\text{RGBN}}(i) \in \text{R}_{\text{color}} \quad (15a) \\ 0 & \text{otherwise} \quad (15b) \end{cases}$$

where $\overline{\text{RGBN}}(i)$ is the mean value of node i in a normalized version of RGB color space, which is a normalized version of RGB with respect to $\text{R} + \text{G} + \text{B}$ (the sum of the values on the R, G, and B color space), and R_{color} is a threshold range. We present the R_{color} in Section V.

We rank all the nodes based on (13), and $\hat{F}^*$ is an N-dimensional vector. Each ranking score indicates the relevance of a node to the objective queries, saliency, and contextual relationship of nodes. Finally, we normalize the vector $\hat{F}^*$ to the range between 0 and 1 (14). Three ranking maps Γ_{red}, Γ_{blue}, and Γ_{yellow} using different specified color queries are constructed, and the results of ranking algorithm are illustrated in Fig. 7. As shown in Fig. 7, using the proposed specified colors and saliency ranking algorithm can decrease the occurrence of false alarm from the original ranking algorithm (11) which is presented in [18]–[22].

TABLE I
ALGORITHM: PROCEDURE OF COMBINING THE INFORMATION OF COLOR, SALIENCY, AND CONTEXTUAL RELATIONSHIP OF NODES

Input: Ω: complete affinity matrix, W: affinity matrix is defined by Eq. (1), S: saliency map is defined by Eq. (3).
Output: $\hat{\Omega}$: complete affinity matrix which combines the information of saliency and contextual relationship of nodes.
Step 1: because all of the nodes belonging to traffic sign regions have high saliency values, the relevances of the i -node and the nodes having low saliency values should be ignored as follows: **if** $S(i) = 0 \quad i \in \{1, \ldots, N\}$, **then** $\hat{\Omega}(j, i) = 0, \quad j = [1, \ldots, N]$, **otherwise** $\hat{\Omega}(i, j) = \Omega(i, j)$.
Step 2: due to the fact that the complex background is liable to affect the ranking results, the relevances of the i-node and unconnected nodes should be ignored as follows: **if** $W(i, k) = 0, \quad i \in \{1, \ldots, N\}, \quad k \in \{1, \ldots, N\}$, **then** $\hat{\Omega}(i, k) = 0$, **otherwise** $\hat{\Omega}(i, k) = \Omega(i, j)$.

D. Traffic Sign Candidate Regions Segmentation

Based on the ranking algorithm, the system gives a ranking score for each node, which indicates how likely it is to be a part of a traffic sign. To segment the traffic sign regions from the results of the ranking algorithm, we propose a multithreshold segmentation algorithm. Each image of ranking result is binarized at a number of different threshold levels, and the connected components at each level are found. Fig. 8 shows the different threshold levels for an example image with the connected components colored. Each connected component

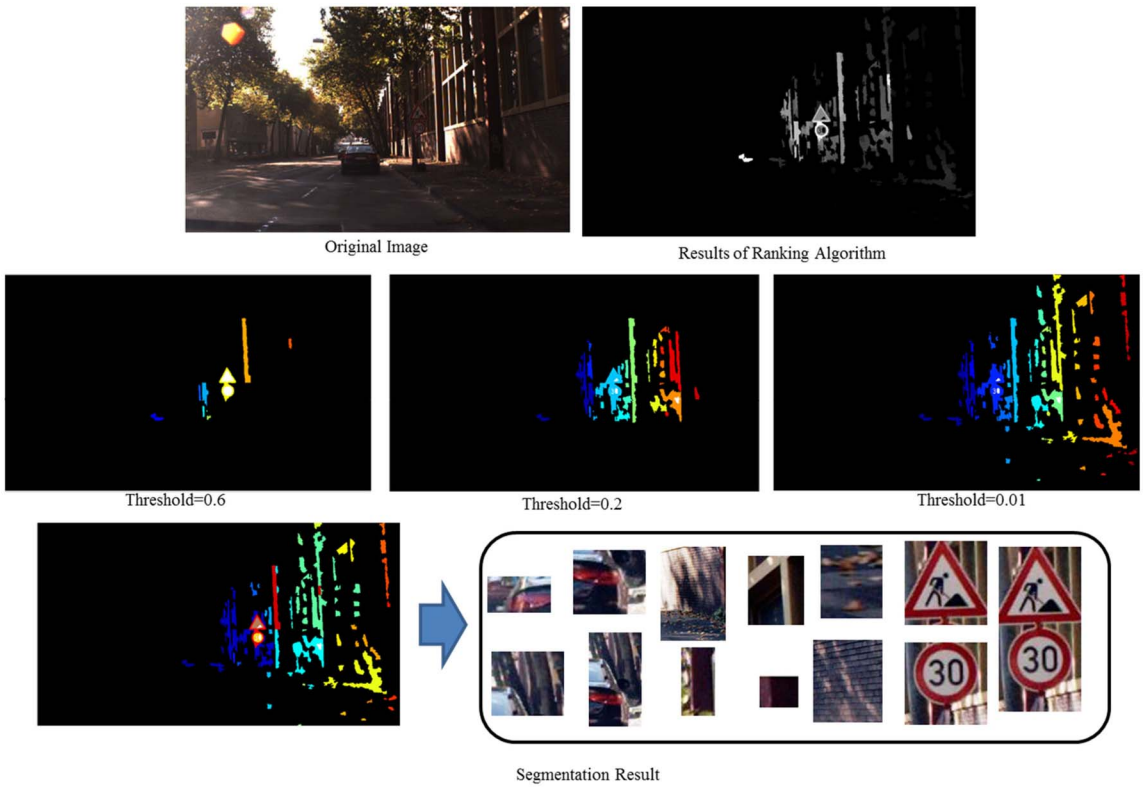

Fig. 8. Process of multithreshold segmentation algorithm.

can be described as L_i^z, which is the ith connected component at level z. Here, $i \in [1, 2, \ldots, N_z]$ and $t \in [1, 2, \ldots, Z]$.

To increase the speed, we threshold only at an appropriate range of values rather than at every possible value, the thresholds are set to 0.6, 0.4, 0.2, and 0.01. Furthermore, we remove the segments with areas that are either too large or small, and cut some segments whose heights are twice as longer as the width. The segmentation results are illustrated in Figs. 2(d) and 8. The threshold TH2 here is set to 1.1 by producing the highest F-measure (see Section V-B).

IV. Traffic Sign Classification Based on SVMs

We implement SVM multiclass classification with linear SVM [24], and use the library LibLinear in our system [26]. The classification stage input is a vector of the HOG descriptor, which Dalal and Triggs [25] proposed for pedestrian detection. On the basis of the gradients of the images, we calculate the different weighted and normalized histograms, overlapping cells with the size of 16×16 pixels, a block size of 4×4 cells, and an orientation resolution of 8. To classify the decision region, all feature vectors of a specific class are grouped together against all vectors corresponding to the remainder of the classes (including noisy objects), according to the one-versus-all classification algorithm.

SVM multiclass classification constructs SVM models. The ith SVM is trained with all the examples in the ith class with positive labels, and all other examples with negative labels. In this paper, the cost of a regularization parameter C is set to 1.2 by producing the highest cross-correlation accuracy.

V. Experiment

To evaluate the effectiveness of the proposed traffic sign detection approach, we carried out a series of comparative experiments using three public traffic sign datasets. The experiments included two components, namely, traffic sign detection and classification. We should note that the primary contribution of this paper is devoted to the traffic sign detection stage. Thus, we have provided more detailed experimental results relating to this stage.

A. Datasets

1) Spanish Traffic Sign Set: Numerous sequences on different routes and under different lighting conditions were captured. Each sequence included thousands of images. With the aim of analyzing the most problematic situations, we use 313 images containing 466 color traffic signs whose size were larger than 30×30 pixels [27], and the traffic signs may be sorted into 19 classes. Eighty-four training images consisted of 191 traffic signs for training. The images presented different detection and recognition problems, such as low illumination, rainy conditions, an array of signs, similar background color, and occlusions. Examples of the Spanish traffic sign set (Spanish) are shown in Fig. 9.

2) GTSDB Dataset: The German traffic sign detection benchmark (GTSDB) dataset [28] contains 900 images of 43 traffic sign classes (divided into 600 training images and 300 evaluation images), Fig. 10 shows several images from this dataset. Three hundred images contain 296 color traffic signs whose sizes were larger than 30×30 pixels. Each image in the

Fig. 9. Examples of the Spanish traffic sign set.

Fig. 10. Examples from the GTSDB.

dataset contains zero to six traffic signs, and they appear from every perspective, as well as under every lighting condition.

3) Summer Swedish Traffic Sign Dataset: The summer Swedish traffic sign (Swedish) dataset [30] was created by recording sequences from over 350 km of Swedish highways and city roads. In total, more than 20 000 frames were recorded in their dataset. The traffic sign regions of the dataset were labeled by the owner, and the traffic signs may be sorted into 49 classes. Set 1 (1970 images containing 2417 traffic signs whose sizes were larger than 15×15 pixels) was used for training. Set 2 (1809 images containing 1136 traffic signs whose sizes were larger than 30×30 pixels) was used for testing. Fig. 11 shows several images from the Swedish dataset. It should be noted that only the traffic sign regions whose sizes were larger than 30×30 were used to verify the proposed system.

B. Experimental Settings

The parameter settings listed in Table II apply to all experiments. α (12), TH1 (Section III-B), and TH2 (Section III-D) are the three parameters that impact the performance of the proposed method. Fig. 12 shows the F-measure rates by varying the values of α, TH1, and TH2 in the GTSDB dataset. The parameters with maximum F-measure rates are selected in our system. It should be noted that in our system, the computational costs do not change significantly if the value of TH1 is varied.

Fig. 11. Examples on the summer Swedish traffic sign dataset.

TABLE II
DEFAULT PARAMETER SETTINGS FOR OUR METHODS

Procedure	Parameter	Value
Eq.(11)	α	0.9
Section III.B	$Th1$	25%
Section III.D	$Th2$	1.1

The effect of illumination changes on color information makes it difficult to find correct thresholds in the basic color spaces (such as RGB) using empirical methods. One solution could be use of a normalized version of RGB with respect to $R + G + B$, as in [27], which uses three normalized components called r, g, and b. We adopt the normalized version of RGB to define the objective vector Y as follows:

$$\text{Red}(i,j) = \begin{cases} \text{True}, & \text{if} \quad \text{r}(i,j) \geq \text{ThR} \\ & \text{and} \quad \text{g}(i,j) \leq \text{ThG} \\ \text{false}, & \text{otherwise} \end{cases}$$

$$\text{Blue}(i,j) = \begin{cases} \text{True}, & \text{if} \quad \text{b}(i,j) \geq \text{ThB} \\ \text{false}, & \text{otherwise} \end{cases}$$

$$\text{Yellow}(i,j) = \begin{cases} \text{True}, & \text{if} \quad (\text{r}(i,j) + \text{g}(i,j)) \geq \text{ThY} \\ \text{false}, & \text{otherwise.} \end{cases}$$

The expressions for each color mask and the threshold range [R_{color} in (15)], which are the same as the RGBNT approach [27], are used in our approach. The threshold values used are shown in Table III.

C. Experiments for Traffic Sign Detection

We label the traffic sign regions on the test set, and use only the traffic signs with a size ranging between 30×30 and 156×193 pixels for evaluation. We use the manually labeled traffic sign regions to evaluate the efficiency of the detection system. It should be noted that only color traffic signs whose sizes are larger than 30×30 pixels are used in this paper. Thus, the number of signs is different from the experiments presented in [8], in which signs whose sizes were larger than 15×15 pixels were evaluated. It should also be noted that

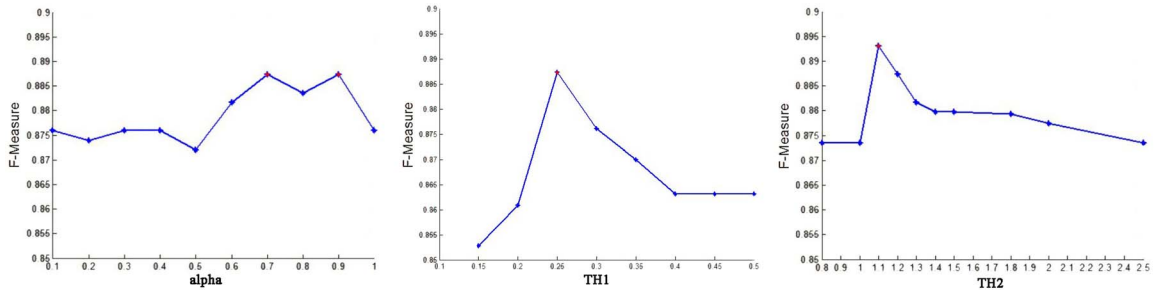

Fig. 12. F-measure rates by varying parameters. α (left), TH1 (middle), and TH2 (right).

TABLE III
THRESHOLD VALUES FOR RGBN, HSI METHODS, AND OURS

Method	Threshold Values
RGBN and ours	$ThR = 0.4, ThG = 0.3, ThB = 0.4, ThY = 0.85$
HSI	$ThR_1 = 10, ThR_2 = 300, ThB_1 = 190, ThB_2 = 270, ThY_1 = 20, ThY_2 = 60, ThY_3 = 150$

TABLE IV
EXPERIMENTAL RESULTS OF THE DIFFERENT DETECTION METHODS ON THE SPANISH TRAFFIC SIGN DATASET

Method	RGBNT	HST	CVS	MSERs	Windows	SDA	Ours
Total number of signs	466	466	466	466	466	466	466
Detections of traffic signs correctly	448	318	378	398	442	287	**450**
Number of false alarm	104	88	68	89	233	**3**	42
Number of misses	18	148	88	68	24	179	**16**
Precision	81.16%	78.33%	84.75%	81.72%	65.48%	**98.97%**	91.46%
Recall	96.14%	68.24%	81.12%	85.40%	94.85%	61.59%	**96.57%**
F-measure	88.02%	72.94%	82.90%	83.52%	77.48%	75.93%	**93.95%**

TABLE V
EXPERIMENTAL RESULTS OF THE DIFFERENT DETECTION METHODS ON THE GTSDB DATASET

Method	RGBNT	HST	CVS	MSERs	Windows	SDA	Ours
Total number of signs	296	296	296	296	296	296	296
Detections of traffic signs correctly	250	203	234	260	**283**	94	260
Number of false alarm	252	245	132	231	288	**15**	30
Number of misses	46	93	62	36	**13**	202	36
Precision	49.80%	45.31%	63.93%	52.95%	49.56%	86.23%	**89.65%**
Recall	84.46%	68.58%	79.05%	87.84%	**95.61%**	31.76%	87.84%
F-measure	62.66%	54.57%	70.70%	65.07%	65.28%	46.42%	**88.73%**

the relationships of the superpixels are used to detect the traffic sign regions. Thus, the traffic regions with smaller sizes (smaller than 30×30) are difficult to detect by the proposed approach.

We evaluate the accuracy of the traffic sign detection by observing the outputs of both detection and classification modules. If we identify the final result as a traffic sign, then we consider it a "detection." If the algorithm fails to detect a sign that is present in the test image, then it is a "miss." Finally, if the system detects a nontraffic-sign object, then it is a "false alarm." Tables IV–VI summarize the results, including the following information: 1) the total number of traffic signs that appear in the test sequence; 2) number of traffic signs that have been correctly detected; 3) number of false alarms in the output of the system; and 4) number of misses.

D. Comparison With State-of-the-Art Traffic Sign Detection Approaches

The proposed approach is compared with the RGBNT algorithm [27], HST algorithm [2], [3], [27], learned color gradient with the constant vote system (CVS) [6], MSERs algorithm [8], [11], sliding window algorithm (window) [10], and graph-based saliency detection algorithm (SDA) [21].

TABLE VI
EXPERIMENTAL RESULTS OF THE DIFFERENT DETECTION METHODS ON THE SUMMER SWEDISH TRAFFIC SIGN DATASET

Method	RGBNT	HST	CVS	MSERs	Windows	SDA	Ours
Total number of signs	1136	1136	1136	1136	1136	1136	1136
Detections of traffic signs correctly	896	809	887	938	989	914	**1093**
Number of false alarm	40	49	1058	**35**	3948	39	42
Number of misses	240	327	249	198	147	222	**43**
Precision	95.73%	94.29%	45.60%	96.40%	20.03%	95.91%	**96.30%**
Recall	78.87%	71.21%	78.08%	82.57%	87.06%	80.46%	**96.21%**
F-measure	86.49%	81.14%	57.58%	88.95%	32.57%	87.51%	**96.25%**

We obtain the detection results by using the same algorithms and parameters that were used in these studies. The threshold values used for RGBNT and HST are shown in Table III based on [27].

E. Detection Results

The results of the comparisons with other algorithms are listed in Tables IV–VI, with the most ideal results marked in bold font. As shown in Tables IV–VI, we may make the following conclusions:

1) The proposed traffic sign detection approach attained the higher *F*-measure rates than the traditional systems making use of color information in [2], [3], and [27]. For example, the proposed approach may, respectively, obtain 5.93% and 21.01% improvement over the RGBNT and the HST on the Spanish traffic sign set, 26.07% and 34.16% improvement over the RGBNT and the HST on the GTSDB dataset, and 9.76% and 15.11% improvement over the RGBNT and the HST on the Swedish traffic sign dataset.
2) The proposed traffic sign detection approach attained higher *F*-measure rates than the traditional systems making use of shape information in [6]. For example, the graph-based ranking and segmentation algorithms can obtain 11.05% improvement over the CVS on the Spanish traffic sign set, 18.03% improvement over the CVS on the GTSDB dataset, and 38.67% improvement over the CVS on the Swedish traffic sign dataset.
3) The proposed traffic sign detection approach attained higher *F*-measure rates than the traditional systems making use of local stability of traffic sign regions in [8] and [11]. For example, the graph-based ranking and segmentation algorithms can obtain 10.43% improvement over the MSERs on the Spanish traffic sign set, 23.66% improvement over the MSERs on the GTSDB dataset, and 7.3% improvement over the MSERs on the Swedish traffic sign dataset.
4) The proposed traffic sign detection approach attained higher *F*-measure rates than the traditional systems making use of the sliding window paradigm of [10]. For example, the graph-based ranking and segmentation algorithms can obtain 16.47% improvement over the sliding window paradigm on the Spanish traffic sign set, 23.45% improvement over the sliding window paradigm on the GTSDB dataset, and 63.68% improvement over the sliding window paradigm on the Swedish traffic sign dataset.
5) The proposed traffic sign detection approach attained higher *F*-measure rates than the traditional graph-based saliency detection approach of [21]. For example, the graph-based ranking and segmentation algorithms can obtain 18.02% improvement over the SDA on the Spanish traffic sign set, 42.31% improvement over the SDA on the GTSDB dataset, and 8.74% improvement over the SDA on the Swedish traffic sign dataset.

F. Classification Results

It should be noted that the Spanish training set consists of 191 traffic signs, which is not sufficient for it to be used as a training set for SVM multiclass classification. In this paper, we combine the training sets of the Spanish dataset, GTSDB dataset, and German TSR benchmark dataset [33], for a total of 43 classes (including noisy objects). We extracted a total of 4369 training images of the noisy object class from the background of the training images. In the Spanish dataset, all the detected traffic signs were classified correctly. The recognition rate of the GTSDB dataset was 97.6343%, and that of the Swedish dataset was 95.4926%.

G. Processing Time

The experiment was performed on a Core i7 QUAD 3.7 GHz with MATLAB 2013, in which the frame dimensions were 1280×960, and JIT-Accelerator and GPU are used to speed up the programs. Specifically, the superpixel generation by the SLIC algorithm take 0.185 s, (about 54%), and the actual saliency measure and ranking algorithm takes 0.062 s. The system speed is around three frames per second. The average processing time of each part is listed in Table VII, and the average processing times of the different detection methods are listed in Table VIII.

H. Discussion

As shown in Tables IV–VI, the number of false alarms decreased markedly using our algorithm. Because the proposed algorithm was an integrated framework of color, spatial,

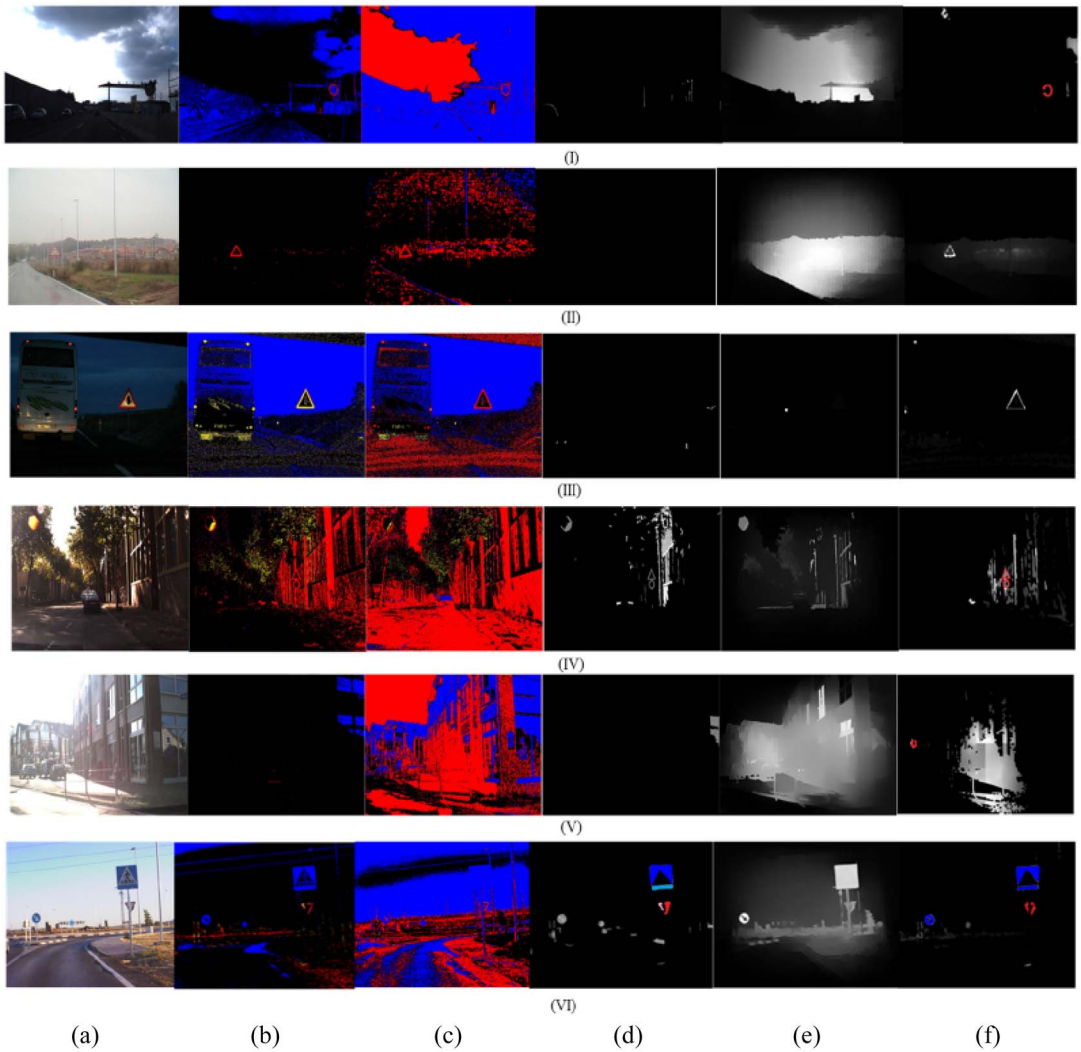

Fig. 13. Segmentation results based on different approaches. (a) Original images. (b) RGBNT. Red, blue, and yellow pixels mean larger values than thresholds on R, G, and B space, and are determined as red, blue, or yellow pixels. (c) HST. Red, blue, and yellow pixels mean larger values than thresholds on H (hue) and S (saturation) components, and are determined as red, blue, or yellow pixels. (d) MSERs. The regions with nonzero gray-scale values are traffic sign candidate regions estimated by MSERs. It should be noted that to emphasize the relationships between segments, we colored several segments. (e) Graph-based saliency detection approach (SDA). (f) Proposed approach. The regions with nonzero gray-scale values are traffic sign candidate regions estimated by the proposed algorithm. To emphasize the efficiency of the multithreshold segmentation algorithm, we colored different segments with different color.

TABLE VII
PROCESSING TIME OF TRAFFIC SIGN DETECTION SYSTEM FOR PER FRAME

SLIC Algorithm and Graph Design	0.185s
Ranking Algorithm with Specified Colors and Saliency	0.062s
Traffic Sign Recognition	0.094s

TABLE VIII
PROCESSING TIMES OF THE DIFFERENT DETECTION SYSTEMS FOR PER FRAME

RGBNT	0.063s
HST	0.074s
CVS	0.513s
MSERs	0.174s
Window	0.966s
SDA	0.316s
Ours	0.341s

saliency, and contextual information for traffic sign detection, it was more discriminative and robust than the algorithms that only use color [see Fig. 13(b) and (c)], shape, local stability [Fig. 13(d)], and saliency information [Fig. 13(e)]. As shown in the images on lines (I), (III), (V), and (VI) of Fig. 13, pixels belonging to the sky were within the threshold range of blue color. Thus, they were detected by the color thresholding algorithms [Fig. 13(a) and (b)]. In contrast, the saliency of the nodes was considered by the proposed algorithm. Thus, the pixels belonging to the sky were not detected by the proposed algorithm.

The number of misses decreased significantly when using the proposed algorithm. As shown in Fig. 13(I) and (V), the gray-scale values of the pixels belonging to the traffic sign region were similar to the backgrounds. Thus, the MSERs algorithms could not detect the traffic signs.

Fig. 13(II) and (III) shows that the edges of the traffic signs were blurry, and the regions at the extremity of the traffic signs were not continuous or monotonic. Thus, the CVS and MSERs algorithms could not detect the traffic signs.

As shown in line (IV) of Fig. 13, using a binary segmentation algorithm, the complex background signified that the traffic sign regions were coherent with the background, such as the RGBNT, HST, and MSERs algorithms, as well as the SDA [Fig. 13(b)–(e)]. In this paper, a score between 0 and 1 was given for each node to describe how likely it would be a part of a traffic sign. We proposed a multithreshold segmentation algorithm, then compared this with the binary segmentation algorithm. It was shown that the multithreshold segmentation could effectively segment the traffic sign candidate regions from a complex background.

Using a binary segmentation algorithm, occlusion signified that a traffic sign was divided into two parts [see line (VI) of Fig. 13(b), (c), (e), and (f)]. In this paper, a multithreshold segmentation algorithm is proposed, which also focused on the components that were not connected with one another, and these were merged based on the criteria. The segmentation algorithm effectively solved the problems of traffic sign detection, such as occlusion, various illumination conditions, and so on.

The proposed algorithm can obtain more than 10% improvement of F-measure, over the traditional graph-based saliency detection approach [SDA, Fig. 13(e)], for the two following reasons.

1) The nodes on the image boundary were used as background seeds in the SDA approach, which made it difficult to distinguish between the traffic sign regions and the background. In contrast with the SDA algorithm for saliency detection, we gave the nodes ranking scores, according to both their spatial structures and their similarities with the specified colors.
2) The binary segmentation approach was used in the SDA approach, in which the traffic sign regions were likely to be coherent with the background.

It should be noted that, as the proposed algorithm utilized color information, we could not use it to detect the traffic signs with a white background, that is why the number of misses using the sliding window algorithm is lower than ours.

VI. Conclusion

In this paper, we described a novel graph-based traffic sign detection approach, which consisted of a saliency measure stage, a graph-based ranking stage, and a multithreshold segmentation stage. We presented a graph with superpixels as nodes for an image, and gave the nodes ranking scores, according to their spatial structures, saliency, contextual relationship of nodes and similarities with the specified colors. We could then segment traffic sign candidate regions with the specified colors from a complex background, on the basis of the multithreshold segmentation algorithm. To verify the effectiveness of the detection module, we tested three traffic sign datasets, that is, the Spanish, GTSDB, and Swedish datasets. The images were captured under different conditions of geometric deformation, damage, weather, and lighting. Different detection algorithms, such as RGBNT, HST, CVS, and MSERs, sliding window classifier, and traditional graph-based SDA algorithms, were used for comparative purposes. The results showed that the proposed method exhibited F-measure rates more than 5% higher than the current state-of-the-art methods. The experimental results were satisfactory even for images containing traffic signs that had been rotated or had undergone occlusion, as well as for images that were photographed under different weather and illumination conditions.

References

[1] X. W. Gao, L. Podladchikova, D. Shaposhnikov, K. Hong, and N. Shevtsov, "Recognition of traffic signs based on their colour and shape features extracted using human vision models," *J. Vis. Commun. Image Represent.*, vol. 17, no. 4, pp. 675–685, 2006.

[2] S. Maldonado-Bascón, S. Lafuente-Arroyo, P. Gil-Jiménez, H. Gómez-Moreno, and F. López-Ferreras, "Road-sign detection and recognition based on support vector machines," *IEEE Trans. Intell. Transp. Syst.*, vol. 8, no. 2, pp. 264–278, Jun. 2007.

[3] S. Maldonado-Bascón, J. Acevedo-Rodríguez, S. Lafuente-Arroyo, A. Fernndez-Caballero, and F. López-Ferreras, "An optimization on pictogram identification for the road-sign recognition task using SVMs," *Comput. Vis. Image Understand.*, vol. 114, no. 3, pp. 373–383, 2010.

[4] M. S. Prieto and A. R. Allen, "Using self-organising maps in the detection and recognition of road signs," *Image Vis. Comput.*, vol. 27, no. 6, pp. 673–683, 2009.

[5] G. Loy, "Fast shape-based road sign detection for a driver assistance system," in *Proc. IEEE Int. Conf. Intell. Robots Syst.*, vol. 1. Sendai, Japan, 2004, pp. 70–75.

[6] S. Houben, "A single target voting scheme for traffic sign detection," in *Proc. IEEE Intell. Veh. Symp. (IV)*, Baden-Baden, Germany, 2011, pp. 124–129.

[7] S. Xu, "Robust traffic sign shape recognition using geometric matching," *IET Intell. Transp. Syst.*, vol. 3, no. 1, pp. 10–18, 2009.

[8] X. Yuan, X. L. Hao, H. J. Chen, and X. Y. Wei, "Robust traffic sign recognition based on color global and local oriented edge magnitude patterns," *IEEE Trans. Intell. Transp. Syst.*, vol. 15, no. 4, pp. 1466–1477, Aug. 2014.

[9] A. Ruta, Y. Li, and X. H. Liu, "Robust class similarity measure for traffic sign recognition," *IEEE Trans. Intell. Transp. Syst.*, vol. 11, no. 4, pp. 846–855, Dec. 2010.

[10] F. Zaklouta and B. Stanciulescu, "Warning traffic sign recognition using a HOG-based K-d tree," in *Proc. Intell. Veh. Symp. (IV)*, Baden-Baden, Germany, 2011, pp. 1019–1024.

[11] J. Greenhalgh and M. Mirmehdi, "Real-Time detection and recognition of road traffic signs," *IEEE Trans. Intell. Transp. Syst.*, vol. 13, no. 4, pp. 1498–1506, Dec. 2012.

[12] Z. Li, C. Dong, L. Zheng, and L. Liu, "Traffic signs detection based on haar-like features and adaboost classifier," in *Proc. ICTIS*, Wuhan, China, 2013, pp. 1128–1135.

[13] K. Lu, Z. M. Ding, and S. Ge, "Sparse-representation-based graph embedding for traffic sign recognition," *IEEE Trans. Intell. Transp. Syst.*, vol. 13, no. 4, pp. 1515–1524, Dec. 2012.

[14] A. de la Escalera, J. M. Armingol, J. M. Pastor, and F. J. Rodriguez, "Visual sign information extraction and identification by deformable models for intelligent vehicles," *IEEE Trans. Intell. Transp. Syst.*, vol. 5, no. 2, pp. 57–68, Jun. 2004.

[15] C. T. Zahn, "Graph-theoretic methods for detecting and describing gestalt clusters," *IEEE Trans. Comput.*, vol. C-20, no. 1, pp. 68–86, Jan. 1971.

[16] F. Pedro and P. H. Daniel, "Efficient graph-based image segmentation," *Int. J. Comput. Vis.*, vol. 59, no. 2, pp. 167–181, 2004.

[17] T. H. Kim, K. M. Lee, and S. U. Lee, "Learning full pairwise affinities for spectral segmentation," *IEEE Trans. Pattern Anal. Mach. Intell.*, vol. 35, no. 7, pp. 1690–1703, Jul. 2013.

[18] D. Zhou, J. Weston, A. Gretton, O. Bousquet, and B. Scholkopf, "Ranking on data manifolds," in *Proc. NIPS*, 2004, pp. 169–176.

[19] D. Zhou, O. Bousquet, T. N. Lal, J. Weston, and B. Scholkopf, "Learning with local and global consistency," in *Proc. NIPS*, 2003, pp. 321–328.

[20] V. Gopalakrishnan, Y. Hu, and D. Rajan, "Random walks on graphs for salient object detection in images," *IEEE Trans. Image Process.*, vol. 19, no. 12, pp. 3232–3242, Dec. 2010.
[21] C. Yang, L. Zhang, H. Lu, X. Ruan, and M. H. Yang, "Saliency detection via graph-based manifold ranking," in *Proc. CVPR*, Portland, OR, USA, 2013, pp. 3166–3173.
[22] C. V. Gustavo, V. B. Tatyana, and D. Zhou, "Semi-supervised graph-based hyperspectral image classification," *IEEE Trans. Geosci. Remote Sens.*, vol. 45, no. 10, pp. 3044–3045, Oct. 2007.
[23] R. Achanta *et al.*, "SLIC superpixels compared to state-of-the-art superpixel methods," *IEEE Trans. Pattern Anal. Mach. Intell.*, vol. 34, no. 11, pp. 2274–2282, Nov. 2012.
[24] C. Cortes and V. Vapnik, "Support-vector networks," *Mach. Learn.*, vol. 20, no. 3, pp. 273–297, 1995.
[25] N. Dalal and B. Triggs, "Histograms of oriented gradients for human detection," in *Proc. CVPR*, vol. 1. San Diego, CA, USA, 2005, pp. 886–893.
[26] C. C. Chang and C. J. Lin, "LIBSVM: A library for support vector machines," *ACM Trans. Intell. Syst. Technol.*, vol. 2, no. 3, pp. 1–27, 2011.
[27] H. Gómez-Moreno, S. Maldonado-Bascón, P. Gil-Jiménez, and S. Lafuente-Arroyo, "Goal evaluation of segmentation algorithms for traffic sign recognition," *IEEE Trans. Intell. Transp. Syst.*, vol. 11, no. 4, pp. 917–930, Dec. 2010.
[28] (2013). *The German Traffic Sign Detection Benchmark*. [Online]. Available: http://benchmark.ini.rub.de/
[29] (2009). *The Spanish Traffic Sign Set*. [Online]. Available: http://agamenon.tsc.uah.es/Segmentation
[30] F. Larsson and M. Felsberg, "Using Fourier descriptors and spatial models for traffic sign recognition," in *Proc. 17th Scand. Conf. Image Anal. (SCIA)*, Ystad, Sweden, 2011, pp. 238–249.
[31] S. Lafuente-Arroyo, P. Garca-Daz, F. J. Acevedo-Rodrłguez, P. Gil-Jimnez, and S. Maldonado-Bascn, "Traffic sign classification invariant to rotations using support vector machines," in *Proc. Adv. Concepts Intell. Vis. Syst.*, 2004, pp. 1–8.
[32] N. Barnes, A. Zelinsky, and L. Fletcher, "Real-time speed sign detection using the radial symmetry detector," *IEEE Trans. Intell. Transp. Syst.*, vol. 9, no. 2, pp. 322–332, Jun. 2008.
[33] J. Stallkamp, M. Schlipsing, J. Salmen, and C. Igel, "Man vs. computer: Benchmarking machine learning algorithms for traffic sign recognition," *Neural Netw.*, vol. 32, no. 8, pp. 323–332, 2011.

Xue Yuan (M'14) received the B.S. degree from Northeastern University, Shenyang, China, and the M.S. and Ph.D. degrees from the Graduate School of Science and Technology, Chiba University, Chiba, Japan, in 2004 and 2007, respectively.

In 2007, she joined SECOM Intelligent Systems Laboratory, Tokyo, Japan, as a Researcher. In 2010, she joined the School of Electronics and Information Engineering, Beijing Jiaotong University, Beijing, China. Her current research interests include image processing and pattern recognition.

Jiaqi Guo received the B.E. degree from the School of Electronics and Information Engineering College, Beijing University of Civil Engineering and Architecture, Beijing, China, in 2012, and the M.E. degree from the School of Electronics and Information Engineering, Beijing Jiaotong University, Beijing, in 2014.

His current research interests include image processing and pattern recognition.

Xiaoli Hao received the B.E., M.E., and Ph.D. degrees from the School of Electronics and Information Engineering, Beijing Jiaotong University, Beijing, China, in 1992, 1995, and 2010, respectively.

She joined the School of Electronics and Information Engineering, Beijing Jiaotong University, in 1995 and became an Associate Professor in 2002. In 2006, she was a Visiting Scholar with the University of California, San Diego, San Diego, CA, USA. Her current research interests include optical imaging, signal processing, and machine vision.

Houjin Chen received the B.E. degree from Lanzhou Jiaotong University, Lanzhou, China, in 1986, and the M.E. and Ph.D. degrees from the School of Electronics and Information Engineering, Beijing Jiaotong University, Beijing, China, in 1989 and 2003, respectively.

He joined the School of Electronics and Information Engineering, Beijing Jiaotong University, in 1989 and became a Professor in 2000. In 1997 and 2000, he was a Visiting Scholar in RICE University, Houston, TX, USA, and the University of Texas, Austin, TX, USA, respectively. He is currently the Dean with the School of Electronics and Information Engineering, Beijing Jiaotong University. His current research interests include signal and information processing, image processing, and simulation and modeling of biological systems.